

● *Contributed Paper*

FLOW AND TRANSPORT STUDIES IN (NON)CONSOLIDATED POROUS (BIO)SYSTEMS CONSISTING OF SOLID OR POROUS BEADS BY PFG NMR

HENK VAN AS,* WYBO PALSTRA,* ULRICH TALLAREK,† AND DAGMAR VAN DUSSCHOTEN*

*Wageningen NMR Centre, Laboratory of Molecular Physics, Wageningen Agricultural University, Wageningen, The Netherlands; and †Institute of Organic Chemistry, University of Tübingen, Tübingen, Germany

Displacement imaging pulsed field gradient nuclear magnetic resonance (PFG NMR) is applied to a number of porous model systems, consisting of either solid or porous particles. By pulsed field gradient nuclear magnetic resonance, the molecular displacement can be measured that occurs during a time interval, Δ , between two consecutive magnetic field gradient pulses. In contrast to conventional techniques, which cover displacements over distances several times the bead diameter, pulsed field gradient nuclear magnetic resonance covers displacements in the order of subpore to several pore distances. Dimensionless scaling is possible based on the root-mean-square displacement normalised on the bead diameter. In solid particles, v and Δ are interchangeable, although different flow regimens are covered. In porous particles, the exchange time between the stagnant mobile phase in the particles and the flowing outside must be taken into account with respect to Δ as well as the porosity. © 1998 Elsevier Science Inc.

Keywords: Dispersive flow; Dimensionless scaling; Flow characteristics; Displacement imaging; Q-Space imaging.

INTRODUCTION

There is a strong interest in the direct and noninvasive measurement of flow and transport processes in complex microporous systems. The understanding of these processes has applications in many fields of research, e.g., (petro-)chemistry, agriculture, environmental sciences, hydrology, biotechnology, and medicine. A thorough understanding of these processes requires information at the void (interparticle space) scale.

Pulsed field gradient nuclear magnetic resonance (PFG NMR) techniques have recently been presented demonstrating the potential to study these processes.^{1–8} By PFG NMR, the molecular displacement can be measured that occurs during a time interval, Δ , between two consecutive magnetic field gradient pulses. In contrast to conventional techniques, which cover displacements over distances several times the bead diameter, PFG NMR covers displacements on the order of subpore to several pore distances. Over these relatively short distances, the characteristics of the flow

change. At distances shorter than the bead diameter it is considered to be stationary random flow, which can be thought to be the sum of unidirectional, more or less time-independent, flow lines with a distribution of the flow direction. At longer distances pseudo-diffusive flow or dispersive flow develops.

It would be advantageous if the fundamentals of flow and transport processes could be studied in upscaled (model) systems with good NMR properties and if the results could be mutually compared via dimensionless scaling. Here we present the results of PFG- or q-space NMR obtained in a number of different systems, consisting of either solid or porous beads and varying bead diameter, and discuss to what extent the results are dependent on characteristic scales (both spatial and temporal) within these models.

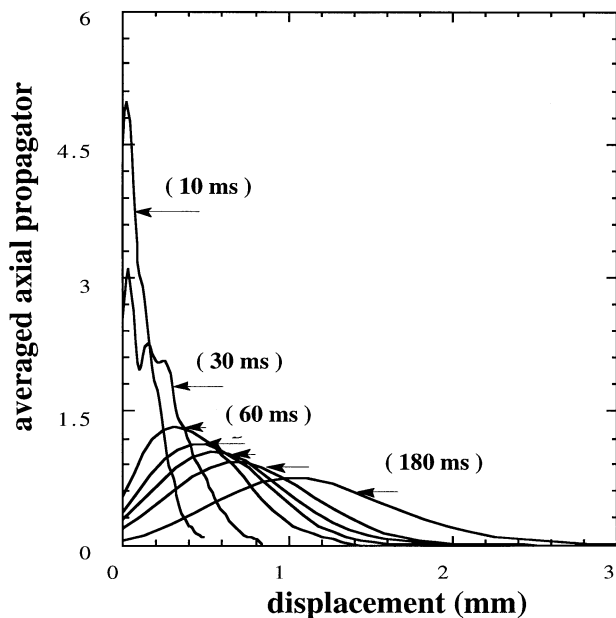
MATERIALS AND METHODS

Flow and transport were studied in a number of different systems: a number of 14-mm inside diameter glass col-

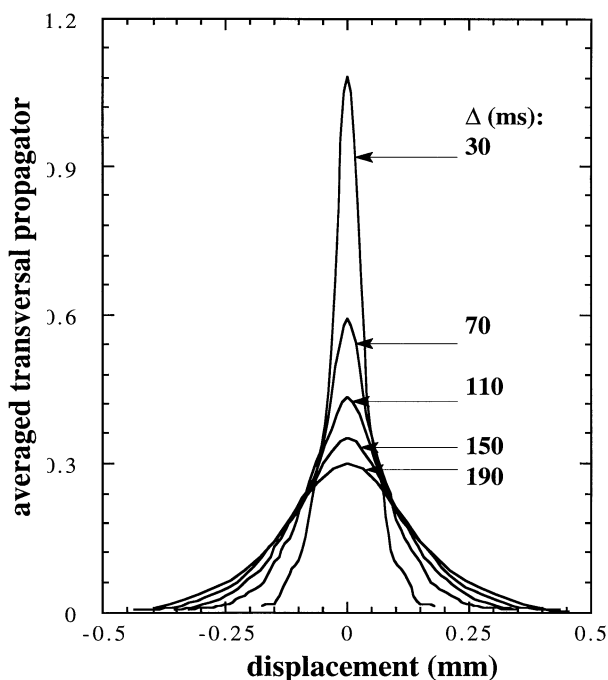
Address correspondence to Dr. H. Van As, Laboratory of Molecular Physics, Wageningen Agricultural University, Dreijenlaan 3, 6703 HA Wageningen, The Netherlands. E-mail:

henk.vanas@water.mf.wau.nl

Present address of Dr. Wybo Palstra: Philips Medical Systems, M&S, Best, The Netherlands



A



B

Fig. 1. Normalised axial (A) and transversal (B) averaged propagator $P(R, \Delta)$ in a glass bead system with a bead diameter of 0.29 mm at different values of Δ . (A) $\langle v \rangle = 6.1$ mm/s; (B) $\langle v \rangle = 4.06$ mm/s.

umns, packed with nonconsolidated, homodisperse, solid glass beads, ranging from 290–1265 μm in diameter; a glass column packed with nonconsolidated, partly porous Sephadex beads (G25/300); a 16-mm inside diameter glass

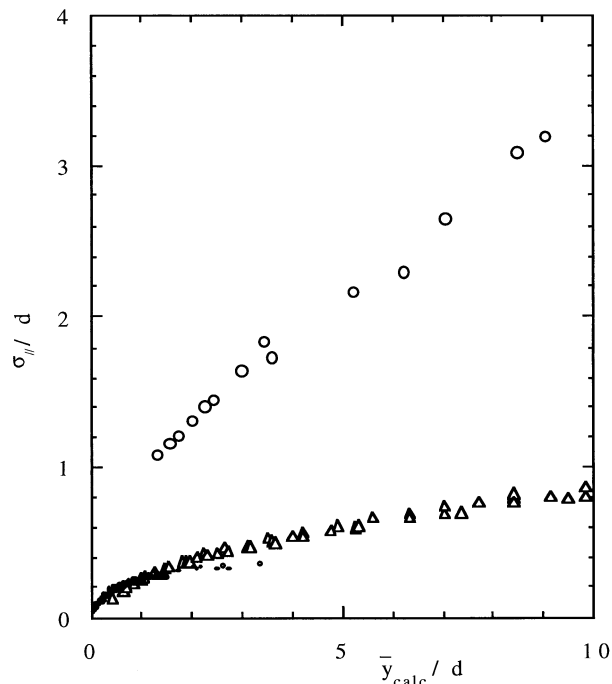


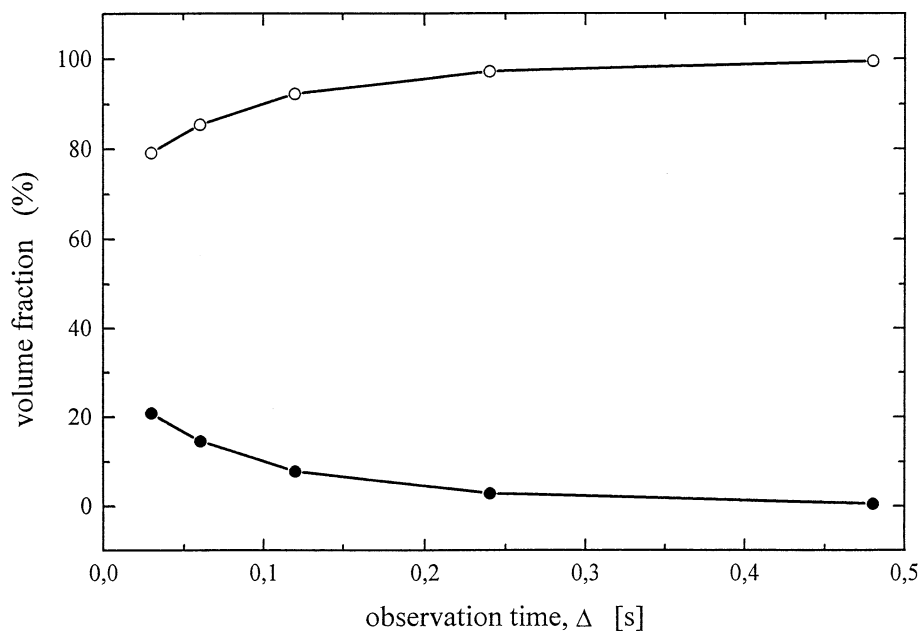
Fig. 2. Normalised axial (a) and transversal (b) rms displacement for glass beads systems with varying bead diameters: $d = 290$ (○), 1347 (*) , 290 (△), and 420–1265 (■) μm .

column packed with nonconsolidated, totally porous, monodisperse, chromatography (C_{18} -silica) particles, with a 50- μm diameter; two 4.4-mm inside diameter PEEK columns packed with either 50- or 15- μm diameter C_{18} -silica particles. The C_{18} -silica particles have interparticle pores with an averaged pore diameter of 120 \AA . Flow was controlled by a precision double syringe high performance liquid chromatography pump. PFG NMR (both spin-echo and stimulated-echo) methods have been used for the measurement of the averaged propagator $P(R, \Delta)$, the probability that a spin at any initial position is displaced by R in the gradient direction over time Δ , the time between the two magnetic field gradient pulses. Typically 64- or 128-G steps have been measured, with δ typically 4 ms or less, and varying Δ . Before Fourier transformation of the complex echo-top amplitudes as a function of $\gamma\delta G$, the dataset was zero filled once. Both transversal (no net flow) and axial flows were studied.

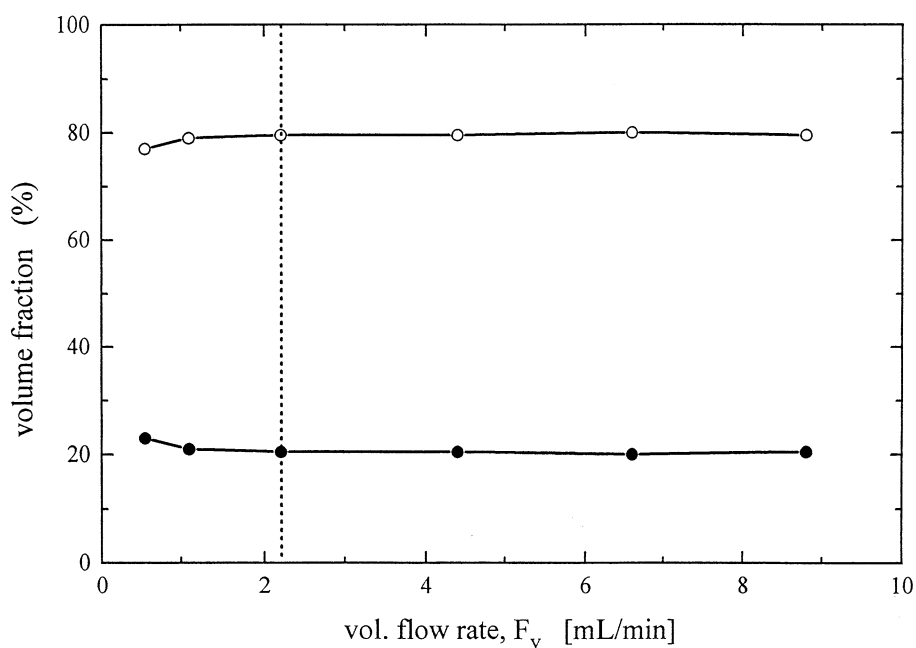
All measurements were performed on a 0.5 T NMR spectrometer, consisting of a SMIS (Guildford, Surrey, UK) console, Bruker (Karlsruhe, Germany) iron core magnet, and DOTY (Columbia, SC, USA) actively shielded gradient and radiofrequency probe.

RESULTS AND DISCUSSION

$P(R, \Delta)$ has been measured for different values of the averaged flow velocity $\langle v \rangle$ and Δ , with the PFG direction



A



B

Fig. 3. Stagnant (●) and net displaced (○) water volume fractions in the porous C_{18} -silica particle system in dependence on Δ at a constant flow rate (2.2 mL/min; A) and in dependence on flow rate at a constant Δ (30 ms; B).

in either the flow (axial) or perpendicular (transversal) the flow direction. Combinations of $\langle v \rangle$ and Δ have been used to cover displacements ranging from less than one to several pore diameters. A set of $P(R, \Delta)$ curves measured in the transversal and the axial direction in the column packed with 290- μm solid glass beads is presented in Fig. 1. At very short displacements (less than

the interpore diameter of $\sim 116 \mu\text{m}$), the shape of the axial propagator is exponential. Increasing the averaged displacement by increasing the observation time, Δ , results in a transition from an exponential to a Gaussian-shaped propagator, which emerges at displacements larger than the bead diameter. At the same time, the exponentially decaying part, the maximum of which is

slightly shifted from zero displacement, is reduced in amplitude and is hardly observed as the averaged displacement is about 1.5 times the bead diameter. The maximum value of the Gaussians shifts to longer displacements and turns out to be equal to the averaged displacement in the flow direction, defined by the product of $\langle v \rangle$ and Δ , where $\langle v \rangle$ is defined by the ratio of the net flux and the effective cross-sectional area available for flow (cross-sectional area times porosity). In the radial direction there is no net displacement, and Gaussian-shaped $P(R, \Delta)$ curves are observed symmetrically around zero displacement. At short displacements these radial propagators turn out to be bi-Gaussian. Based on the width of these Gaussians one can calculate the dispersion coefficients. The smallest fraction represented a constant dispersion coefficient of about 4 times the diffusion coefficient, and the largest fraction represented a dispersion coefficient that increased with increasing averaged axial displacement. The amplitude of the smallest fraction decreased to zero at increasing $\langle v \rangle$ and Δ .

It is clearly observed from the results that the dispersion coefficient D_p depends on Δ , reflecting different flow regimens. By consequence, dimensionless scaling, e.g., by plotting the ratio of D_p and the molecular diffusion coefficient D_s versus the dimensionless Peclet number, Pe , does not hold for these results.⁹ Pe is defined as:

$$Pe = \langle v \rangle d(1 - p)/(pD_s), \quad (1)$$

where d is the particle diameter, and p is the porosity of the system. In Fig. 2 we present a plot of the root-mean-square (rms) displacement $\sigma = (2D_p\Delta)^{1/2}$ divided by d versus the averaged net axial displacement ($= \langle v \rangle \Delta$), also normalised on d . This plot contains data obtained with different solid glass bead diameters, $\langle v \rangle$ and Δ .

These results demonstrate that for systems consisting of nonconsolidated, solid particles, $\langle v \rangle$ and Δ are interchangeable. Although different flow behaviour is observed at different values of Δ , reflected by the different shapes of the average propagator, (rms) displacements can be scaled to the bead diameter, demonstrating that the bead diameter reflects a characteristic length for flow in these systems. This scaling breaks down when the ratio between the diameter of the cylinder containing the particles and the particle diameter is less than about 15.

In consolidated solid systems, including dead ends, and in porous particle systems, $\langle v \rangle$ and Δ are no longer interchangeable as long as a stagnant fluid phase is observed. The observation of the stagnant mobile phase in the porous beads or in the dead ends, with a symmetrical averaged propagator around zero, depends on Δ and the bead diameter, not on $\langle v \rangle$.¹⁰ This is nicely demonstrated for the 50- μm porous C_{18} -silica particle system in

Fig. 3, where the volume fractions of the stagnant and flowing fluid are given as a function of $\langle v \rangle$ (Fig. 3a) or of Δ (Fig. 3b). This behaviour is due to the exchange of water between the intraparticle and/or deadend space and the interparticle space.¹⁰ As a result the effective porosity for the flowing fluid phase as observed by NMR depends on Δ : $p_{\text{nmr}} = p_{\text{inter}} + fp_{\text{intra}}$, where $f = 1 - \exp(-\Delta/t_{\text{exch}})$, and t_{exch} is the residence time of water in the beads.¹⁰ The results of dispersive flow measurements in porous particles fit within the results for solid beads as presented in Fig. 2 if σ is corrected for this exchange behaviour by taking $\sigma(p_{\text{inter}}/p_{\text{nmr}})$, where p_{inter} can be considered the limiting value of p_{nmr} for $\Delta = 0$.

In complex systems where more than one particle-related water fraction is present these fractions can also be separated based on a combination of D and T_2 information,¹¹ as has been demonstrated in the Sephadex system.¹²

Acknowledgments—This research was supported in part by Grant 87010 AG from Koninklijke/Shell Laboratory Amsterdam and Koninklijke/Shell Exploration and Production Laboratory Rijswijk and by EU-Human Capital and Mobility Grant ERBCHGECT 940061.

REFERENCES

1. Schaafsma, T.J.; Van As, H.; Palstra, W.D.; Snaar, J.E.M.; de Jager, P.A. Quantitative measurement and imaging of transport processes in plants and porous media by ^1H NMR. *Magn. Reson. Imag.* 10:827–836; 1992.
2. Rajanayagam, V.; Yao, S.; Pope, J. Quantitative magnetic resonance flow and diffusion imaging in porous media. *Magn. Reson. Imag.* 13:729–738; 1995.
3. Kutchovsky, Y.E.; Scriven, L.E.; Davis, H.T.; Hammer, B. NMR imaging of velocity profiles and velocity distributions in bead packs. *Phys. Fluids.* 8:863–870; 1996.
4. Lebon, L.; Oger, L.; Leblond, J.; Hulin, J.P.; Martys, N.S.; Schwartz, L.M. Pulsed gradient NMR measurements and numerical simulation of flow velocity distribution in sphere packings. *Phys. Fluids* 8:293–301; 1996.
5. Packer, K.J.; Tessier, J.J. The characterization of fluid transport in a porous solid by pulsed gradient stimulated echo NMR. *Mol. Phys.* 87:267–272; 1996.
6. Seymour, J.D.; Callaghan, P.T. Generalized approach to NMR analysis of flow and dispersion in porous media. *AIChE J.* 43:2096–2111; 1997.
7. Tallarek, U.; Albert, K.; Bayer, E.; Guiochon, G. Measurement of transverse and axial apparent dispersion coefficients in packed beds. *AIChE J.* 42:3041–3053; 1996.
8. Tessier, J.J.; Packer, K.J.; Thovert, J.-F.; Adler, P.M. NMR measurements and numerical simulation of fluid transport in porous solids. *AIChE J.* 43:1653–1661; 1997.
9. Han, N.-W.; Bhakta, J.; Carbonell, R.G. Longitudinal and lateral dispersion in packed beds: effect of column length and particle size distribution. *AIChE J.* 31:277–284; 1985.

10. Tallarek, U.; Van Dusschoten, D.; Van As, H.; Guiochon, G.; Bayer, E. Mass transfer in chromatographic columns studied by pulsed field gradient NMR. *Magn. Reson. Imaging* 16:699-702;1998.
11. Van Dusschoten, D.; de Jager, P.A.; Van As, H. Extracting diffusion constants from echo-time dependent PFG NMR data using relaxation time information. *J. Magn. Reson.* A116:22-28; 1995.
12. Van Dusschoten, D. Probing water motion in heterogeneous systems: a multi-parameter approach. Ph.D. Dissertation. Wageningen, The Netherlands: Wageningen Agricultural University; 1995.